ISSN:1687-1006

The Egyptian International Journal of Engineering Sciences and Technology

Vol. 27 (2019) 12–22

http://www.eijest.zu.edu.eg

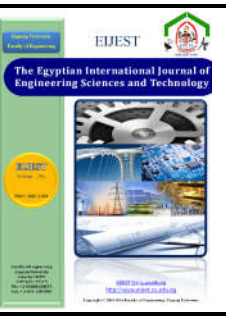

Finite Element Analysis of Double Wishbone Vehicle Suspension System

Ayman E. Nabawy*, Alaa A. Abdelrahman, Ayman M. Abdelhaleem, Soliman. S. Alieldin

Mechanical Design & Production Engineering Dept., Faculty of Engineering, Zagazig University, P.O. Box 44519, Zagazig, Egypt.

ARTICLE INFO

Article history:
Received 15 November2018
Received in revised form
00 November 2018
Accepted 30 December 2018
Available online 00 January 2019

Keywords:
Double wishbone suspension
Links flexibility
Finite element
Revolute joint
Material damping
Road bump
Viscoelastic
Timoshenko beam theory(TBT).

ABSTRACT

Suspension systems play an important role in vehicles. These systems provide passenger comfort and vibration isolation from road bumps. Thus an efficient finite element model is required to study and analyze the dynamic response of these suspension systems. This paper presents a finite element model to analyze the dynamic response of double wishbone vehicle suspension system taking into consideration both links and joints flexibilities. Links are modeled using plane frame element based on Timoshenko beam theory (TBT) kinematic relations. On the other hand, the revolute joint element, developed in ANSYS, is adopted to model joints flexibility.Both internal viscoelastic and external viscous as well as the modal proportional damping models are adopted to simulate the damping effect. The resulting dynamic finite element equations of motion are solved using Newmark numerical technique. The proposed numerical methodology is checked by comparing the obtained results with the developed analytical solution and good agreement is noticed. The applicability of the proposed procedure is demonstrated by operating parametric studies to illustrate the effects of the road irregularity configurations, the vehicle travelling velocity, as well as the material damping on the dynamic response characteristics of the double wishbone suspension system. The obtained results are helpful for the mechanical design of these structural systems.

1. Introduction

Vehicle suspension systems have an essential role in vehicles dynamics. These systems provide passenger comfort and prevent noises and vibrations transmission into vehicle body, Reimpellet al. [2001]. Moreover, these systems provide stability and safe braking of vehicles as well as improve the handling capabilities, Jazar [2017]. Additionally, these suspension systems prevent vehicles from damage and wear failure, Blundell and Harty [2015].

According to the left and right wheel independency, suspension systems are classified to dependent and independent suspension systems. The independent double wishbone suspension system is considered one of the most commonly type used in vehicles, Cheng and Lin [2014].

The lower control arm, known as A-type arm, is considered to be one of the most effective parts in the suspension systems. This A- type arm attains the desired position for wheels and it provides safe up and down wheel motion, Rutci [2015]. Additionally, it is considered as the most critically loaded partr in the suspension system,Patil et al. [2013].An effective stress analysis procedure is essentially needed to avoid failure of the A-type arm, throughout stress analysis procedure, both the dynamic forces as well as dynamic deflections are investigated, Dehkordi

* Corresponding author. Tel.: 01555517800, 01143852712.
E-mail address: *eng.nabawy.2010@Gmail.com*

[2014]. It is difficult of investigate the dynamic behavior of such suspension systems with both links and joints flexibilities, analytically.Consequently,an effective numerical procedure is required to study and analyze the dynamic behavior of these systems.Finite element procedure is one of the most common numerical techniques used to study and analyze such systems.

Rubber bushings are essential in suspension systems to connect the suspension links together and consequently with vehicle body. These rubber bushings connectors are supportive in shock absorption during motion over road irregularities,Azadi and Forouzesh[2011].The kinematics analysis of both double wishbone and MacPherson suspension systems are investigated using a complete spatial model, Reddy et al. [2016]. Incorporating the effects of linkage configuration on the kinematic and dynamic performances of suspension, suspension linkages are analyzed using a kineto-dynamic quarter-car model, Balike et al. [2011]. The kinematic performance of the double wishbone suspension system is analytically analyzed usinga complete kinematic model to define the essential kinematic parameters such as camber, caster, kingpin, toe angles, and track variation,Tanik, and Parlaktas [2015]. On the other hand, safe limits in toe and camber angles as well as the wheel travel of the vehicle experiencing a bounce and rebound due to a bump are investigated, Bhoraskar et al. [2017]. The handling characteristics of vehicle are improved and the camber and Toe angles of the double wishbone suspension system are controlled through adaptive variable length arms, Kavitha et al. [2018]. New suspension, unsprung mass, and compliance parameters are incorporated to investigate the dynamic behavior investigateusing a linear quarter car model, Kanchwala and Chatterjee [2017]. Base on variable camber angle, a passive double wishbone suspension system is designed and analyzed, Pourshams et al. [2011]. The time effect on life cycle analysis of a car is illustrated through dynamic procedure,Soo et al. [2015].

Many research papers focused on the analysis and design of the lower control A-type arm. Using both finite element and experimental studies, the dynamic and the vibrational fatigue damage behaviors of the lower A-type arm are analyzed, Kadhim et al. [2011]. The finite element methodology is applied to obtain a complete stress analysis of the lower control A-type arm of the double wishbone vehicle suspension system,Nithin and Veeresha [2013]. To improve the design procedure of the A-type control arm and overcome problems associated with vehicle weight, A-type control arm made of composite materials should be used. The finite element method (FEM) is applied to study and analyze stress and strains in lower control arm made of carbon fiber polymer, Patil et al. [2013]. To minimize the induced stresses and loads, a complete static, dynamic and optimization analyses of the A-type control arm are discussed, Dehkordi [2014]. Using both FEM and experimental studies using computerized universal testing machine of 25 ton capacity,the working life of the A-type control arm is investigated,Gadade and Todkar [2015].Considering the damping effect of the vehicle tire, a detailed nonlinear quarter car suspension model is proposed to detect kinematic variables of sprung mass as well as the lower A-type control arm, Abdelsalam et al. [2016].Using the FEM, both static and dynamic behaviors of the suspension system are studied and analyzed, Ijagbemi et al. [2016].Applying the FEM, the buckling strength of the lower A-type control arm is investigated, Sridharan and Balamurugan [2016].A comparative study of composite and steel A-type lower control arms is conducted using FEM to investigate the benefits of using composite material in manufacturing process of lower control arms over the classical elastic one in suspension systems, Ramesh et al. [2017].

This paper presents a finite element model capable of studying and analyzing the double wishbone vehicle suspension system incorporating flexibilities of suspension links as well as connecting joints. To investigate the effect of material damping on the dynamic response of the double wishbone vehicle suspension system, different damping models are considered. The internal viscoelastic, the external viscous, as well as the modal proportional damping models are considered. The proposed numerical procedure is verified by comparing the obtained results with the analytical solution. Parametric studies are conducted to investigate the effects of the different suspension and vehicle parameters on the dynamic behavior of the double wishbone suspension systems.

2. Formulation of the problem

Within this section, the mathematical formulation of the problem is presented. Consider the quarter car mode shown in Fig. 1. According to the proposed

planar model all links of the suspension system are modeled as a plane frame structural element while the revolute joints are modeled with flexible translational springs for the translational degrees of freedom in both *x* and *y* directionswhile a torsional spring is used for the rotational degree of freedom about z axis. On the other hand, both tire and strut AB are presented by a vertical translational springs. Both upper and lower control arms are modeled using either elastic or viscoelastic materials while the revolute flexible joints are modeled with elastic materials. The motion of the tire over the road bump,$y(t)$provides a vertical excitation for the body of the vehicle. Both step and sinusoidal road bump profiles are considered. The problem formulation can be presented as follows:

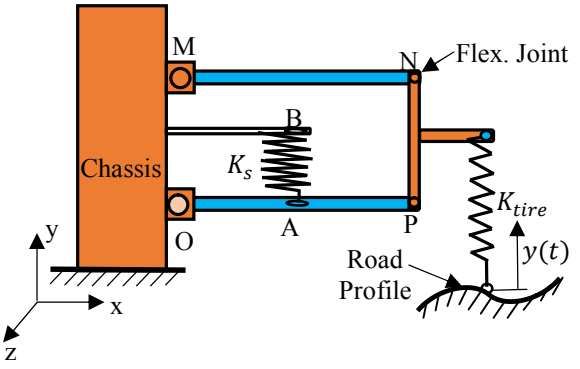

Fig. 1. Quarter-car model of a double wishbone suspension.

2.1. The displacement field and the kinematic relations

The displacement field according to Timoshenko beam theory (TBT) is written as, Reddy [2007]

$$\boldsymbol{u_x(x,t) = u(x,t) + y\phi_x(x,t)\ \ and}$$
$$\boldsymbol{u_y(x,t) = w(x,t)} \qquad (\mathbf{1})$$

where*u* is the axial displacement, *w* is the transverse deflection, and ϕ_x denotes the rotation of the cross section about the z-axis. The strain field can be expressed as, Reddy [2011]

$$\varepsilon_x(x,t) = \frac{\partial u_x(x,t)}{\partial x} = \frac{\partial u(x,t)}{\partial x} + z\frac{\partial \phi_x(x,t)}{\partial x} \qquad (2)$$

$$\gamma_{xy}(x,t) = \frac{\partial u_x(x,t)}{\partial y} + \frac{\partial u_y(x,t)}{\partial x} \qquad (3)$$

whereε_{xx} and γ_{xz} refer to the normal and shear strain components; respectively.

2.2. Stress strain constitutive law

The internal viscoelastic, the external viscous as well as the modal proportional damping are considered to investigate the effect of damping on the dynamic characteristics of vehicle suspension system. Both elastic and viscoelastic stress strain relations are presented in this section.

2.2.1. Constitutive relations of elastic materials

The stress–strain relation for linear isotropic homogenous elastic materials can be written as, Carrera et al. [2011]

$$\sigma_x(x,t) = E\varepsilon_x(x,t) \qquad (4)$$

$$\tau_{xz}(x,t) = \kappa_s G\gamma_{xz}(x,t) \qquad (5)$$

where$G$ the shear modulus$[G = 0.5E/(1+v)]$, k_s is the shear correction factor, and v is Poisson's ratio.

2.2.2. Constitutive relations of viscoelastic materials

Assuming linear isothermal isotropic homogeneous viscoelastic materials, the stress response over time domain [-∞, t] is found by means of the principle of superposition. In this view, the principle argues that the total stress resulting from a sequence of applied strains is equal to the sum of the stresses due to the individual strains from time $t = -\infty$ till the current time t. This is represented by the following hereditary integral, Findley et al. [2013]:

$$\sigma_x(x,t) = \int_{-\infty}^{t} E(t-s)\frac{\partial \varepsilon_x(x,s)}{\partial s}ds$$
$$= E(0)\varepsilon_x(x,t) - \int_0^t \frac{dE(t-s)}{ds}\varepsilon_x(x,s)ds \qquad (6)$$

$$\tau_{xz}(x,t) = \int_{-\infty}^{t} \kappa_s G(t-s)\frac{\partial \gamma_{xz}(x,s)}{\partial s}ds$$
$$= \kappa_s G(0)\gamma_{xz}(x,t)$$
$$- \kappa_s \int_0^t \frac{dG(t-s)}{ds}\gamma_{xz}(x,s)ds \qquad (7)$$

where$E(t)$ and $G(t)$ refer to the relaxation and shear moduli of the viscoelastic material; respectively. Considering the Wiechert viscoelastic mechanical model, the relaxation and shear moduli can be expressed as;

$$E(t-s) = E_\infty + \sum_{n=1}^{N} E_n \left(e^{\frac{-(t-s)}{\rho_n}}\right) and\ \ G(t-s) = G_\infty + \sum_{n=1}^{N} G_n \left(e^{\frac{-(t-s)}{\rho_n}}\right) \quad (8)$$

2.3. Equations of motion

According to TBT, the equation of motion can be expressed as, Martin [2016]

$$E(0)A\frac{\partial^2 u(x,t)}{\partial x^2} - A\int_0^t \frac{dE(t-s)}{ds}\frac{\partial^2 u(x,s)}{\partial x^2}ds + f = \rho A\frac{\partial^2 u(x,t)}{\partial t^2} \quad (9a)$$

$$k_s AG(0)\left(-\frac{\partial \phi(x,t)}{\partial x} + \frac{\partial^2 w(x,t)}{\partial x^2}\right) - k_s A\int_0^t \frac{dG(t-s)}{ds}\left(-\frac{\partial \phi(x,s)}{\partial x} + \frac{\partial^2 w(x,s)}{\partial x^2}\right)ds + q = \rho A\frac{\partial^2 w(x,t)}{\partial t^2} \quad (9b)$$

$$IE(0)\frac{\partial^2 \phi(x,t)}{\partial x^2} + k_s AG(0)\left(-\phi(x,t) + \frac{\partial w(x,t)}{\partial x}\right) - \left(I\int_0^t \frac{dE(t-s)}{ds}\frac{\partial^2 \phi(x,s)}{\partial x^2}ds + k_s A\int_0^t \frac{dG(t-s)}{ds}\left(-\phi(x,s) + \frac{\partial w(x,s)}{\partial x}\right)ds\right) = \rho I\frac{\partial^2 \phi(x,t)}{\partial t^2} \quad (9c)$$

By the same way, the equation of motion for viscously damped TB, can be written as, Weili et al. [2013], Inman [2014]

$$EA\frac{\partial^2 u(x,t)}{\partial x^2} + f = \rho A\frac{\partial^2 u(x,t)}{\partial t^2} + C_v\frac{\partial u(x,t)}{\partial t} \quad (10a)$$

$$k_s AG\left(-\frac{\partial \phi(x,t)}{\partial x} + \frac{\partial^2 w(x,t)}{\partial x^2}\right) + q = \rho A\frac{\partial^2 w(x,t)}{\partial t^2} + C_v\frac{\partial w(x,t)}{\partial t} \quad (10b)$$

$$IE\frac{\partial^2 \phi(x,t)}{\partial x^2} + k_s AG\left(-\phi(x,t) + \frac{\partial w(x,t)}{\partial x}\right) = \rho I\frac{\partial^2 \phi(x,t)}{\partial t^2} + C_v\frac{\partial \phi(x,t)}{\partial t} \quad (10c)$$

where A, I, C_v, f, and q are the beam cross section area, the area moment of inertia, the viscous damping coefficient, and the uniformly distributed loads.

3. Evaluation of the VE convolution integral

To develop an incremental recursive form for the VE constitutive relations which is more suitable for finite element implementation. Assume the time domain is divided into time steps each of intensity$\boldsymbol{\Delta t}$. Moreover, assume that the time response is knownat $(\boldsymbol{t-\Delta t})$. To obtain the VE response at time the normal stress can be expressed as

$$\sigma_x(x,t) = E(0)\varepsilon_x(x,t) - \sum_{n=1}^{N}\int_0^t \frac{E_n}{\rho_n}\left(e^{\frac{t-s}{\rho_n}}\right)\varepsilon_x(x,s)ds = E(0)\varepsilon_x(x,t) - \sum_{n=1}^{N} I_n(x,t) \quad (11)$$

The integration $I_n(\mathrm{x},t)$ could be approximated as

$$I_n(x,t) = \frac{E_n}{\rho_n}\int_0^{\Delta t} \varepsilon_x(x,t-s)\left(e^{\frac{-s}{\rho_n}}\right)ds + \frac{E_n}{\rho_n}\int_{\Delta t}^{t} \varepsilon_x(x,t-s)\left(e^{\frac{-s}{\rho_n}}\right)ds \quad (12)$$

The first term in Eq. (12) can be simplified using the trapezoidal rule as

$$\frac{E_n}{\rho_n}\int_0^{\Delta t} \varepsilon_x(x,t-s)\left(e^{\frac{-(s)}{\rho_n}}\right)ds = \frac{E_n}{\rho_n}\left(e^{\frac{-t}{\rho_n}}\right)\left(\begin{array}{c}\rho_n\left[\begin{array}{c}\left(\varepsilon_x(x,t)\left(e^{\frac{t}{\rho_n}}\right)\right)\\ -\varepsilon_x(t-\Delta t)\left(e^{\frac{t-\Delta t}{\rho_n}}\right)\end{array}\right]\\ -\int_{t-\Delta t}^{t}\frac{\partial \varepsilon_x(x,\eta)}{\partial \eta}\rho_n\left(e^{\frac{\eta}{\rho_n}}\right)d\eta\end{array}\right) \quad (13)$$

Simplifying Eq. (13) yields;

$$\frac{E_n}{\rho_n}\int_0^{\Delta t}\varepsilon_x(x,t-s)\left(e^{\frac{-(s)}{\rho n}}\right)ds$$

$$\cong\frac{E_n}{\rho_n}\begin{pmatrix}\varepsilon_x(x,t)\left[\rho_n-\frac{\rho_n^2}{\Delta t}\right]\left(1-e^{\frac{-\Delta t}{\rho_n}}\right)\\+\varepsilon_x(x,t-\Delta t)\begin{bmatrix}-\rho_n e^{\frac{-\Delta t}{\rho_n}}\\+\frac{\rho_n^2}{\Delta t}\left(1-e^{\frac{-\Delta t}{\rho_n}}\right)\end{bmatrix}\end{pmatrix}\quad(14)$$

The second term in Eq. (12) can be simplified as

$$\frac{E_n}{\rho_n}\int_{\Delta t}^{t}\varepsilon_x(x,t-s)\left(e^{\frac{-s}{\rho n}}\right)ds=$$
$$=\left(e^{\frac{-\Delta t}{\rho n}}\right)h_n(x,t-\Delta t)\quad(15)$$

Thus the constitutive relation can be written as

$$\sigma(x,t)=\sigma^c(x,t)+\sigma^h(x,t)\quad(16)$$

where

$$\sigma^c(x,t)=\left(E_\infty+\sum_{n=1}^{n}E_n\left[\frac{\rho_n}{\Delta t}\left(1-e^{\frac{-\Delta t}{\rho_n}}\right)\right]\right)\varepsilon(x,t)$$
$$=E_{ve}\,\varepsilon(x,t)\quad(17a)$$

and

$$\sigma^h(x,t)$$
$$=\sum_{n=1}^{N}E_n\begin{pmatrix}-e^{\frac{-\Delta t}{\rho_n}}+\frac{\rho_n}{\Delta t}\left(1-e^{\frac{-\Delta t}{\rho_n}}\right)\varepsilon(x,t-\Delta t)\\+e^{\frac{-\Delta t}{\rho_n}}h_n(x,t-\Delta t)\end{pmatrix}\quad(17b)$$

with

$$h_n(x,t)$$
$$=E_n\begin{pmatrix}\varepsilon(x,t)\left[1+\frac{\rho_n}{\Delta t}\left(1-e^{\frac{-\Delta t}{\rho_n}}\right)\right]+\\\varepsilon(x,t-\Delta t)\left[-e^{\frac{-\Delta t}{\rho_n}}+\frac{\rho_n}{\Delta t}\left(1-e^{\frac{-\Delta t}{\rho_n}}\right)\right]\end{pmatrix}$$
$$+e^{\frac{-\Delta t}{\rho_n}}h_n(x,t-\Delta t)\quad(17c)$$

Similar expressions can be derived for the VE shear modulus.

4. Finite element Formulation

The domain of the problem of divided into finite elements. Both two and three nodded isoparametric TB elements can be used, Capsoni et al. [2013]. The revolute joint element developed in ANSYS, Kohnke [1997] is adopted for joint flexibility. Applying the principle of virtual work, the dynamic finite element equations of motion of the viscoelastic Timoshenko beam, VETB can be written as

$$\int_v\delta\varepsilon_x^T\sigma_x dv+\int_v\delta\gamma_{xy}^T\tau_{xy}dv$$
$$=-\int_v\rho\delta U^T\ddot{U}dv$$
$$+\int_0^L\begin{bmatrix}\delta u_0^T P_x+\delta w^T P_y\\+\delta\phi^T m\end{bmatrix}dx\quad(18)$$

where P_x, P_y, and m refer to the distributed normal, shear and bending moment while ρ is the mass density. Equation (18) can be rewritten as

$$\int_0^L\int_A\left[\delta\varepsilon_x^T\sigma_x+\delta\gamma_{xy}^T\tau_{xy}\right]dAdx$$
$$=-\int_0^L\int_A\rho\delta U^T\ddot{U}dAdx$$
$$+\int_0^L\left[\delta u_0^T P_x+\delta w^T P_y\right.$$
$$\left.+\delta\phi^T m\right]dx\quad(19)$$

Substituting from both kinematic relations and stress strain relations into Eq. (19) yields;

$$[R]^T[M_l^e][R]\{\ddot{q}\}+[R]^T[K_l^e][R]\{q\}=[R]^T\{F_{ext}\}^e$$
$$-[R]^T\{F_{ve}\}^e\quad(20a)$$

Also, the dynamic finite element equation of motion for viscously damped TBT can be expressed in global coordinates as

$$[R]^T[M_l^e][R]\{\ddot{q}\}+[R]^T[C_l^e][R]\{\dot{q}\}$$
$$+[R]^T[K_l^e][R]\{q\}=[R]^T\{F_{ext}\}^e\quad(20b)$$

where $[M_l^e]$, $[K_l^e]$, $[C_l^e]$, $[R]$, and $\{F_{ve}\}^e$ are the element mass, stiffness, and viscous damping, transformation matrices and the force vector due to viscoelastic material history; respectively.These matrices and vector are defined by the following equation:

$$[K_l^e]=\int_{-1}^{1}B^T[E_{ve}][B]|J|d\xi,\quad\{F_{ve}\}^e$$
$$=\int_v B^T\{\sigma^h\}^e dv,[C_l^e]=\int_{-1}^{1}C_v[N]^T[N]|J|d\xi$$
$$and\ \ [M_l^e]=\int_{-1}^{1}\rho[N]^T[N]|J|d\xi\quad(21)$$

where [N] and [B] are the shape function strain displacement relation matrix; respectively. Considering the revolute joint element, the element stiffness, viscous damping, and mass matrix of COMBIN7 as expressed in ANSYS.

5. Validation of the numerical procedure

To check the validity of the developed numerical procedure, consider a simply supported TB subjected to a uniformly distributed load of intensity q as shown in Fig. 2a. To consider the joint flexibility, the roller support is modelled as a vertical translational spring with stiffness, k_y while the hinged support is modelled by two horizontal and vertical translational springs with stiffness's k_x and k_y respectively, as shown in Fig. 2b, Da Costa Azevêdo [2016].The intensity the distributed load$q_0 = 100\ N/m$.The beam has a length of$L = 4\ m$, width,$b = 0.2\ m$ and height,$h = 0.4\ m$.$k_x$andk_y are taken to be $1.75 * 10^{11}\ N/m$. The modulus of elasticity, mass density, shear correction factor, and Poisson's ratio are taken to be$E = 9.8 * 10^7 Pa$,$\rho = 500\ kg/m^3$, $ks = 0.8333$ and$v = 0.3$, respectively.

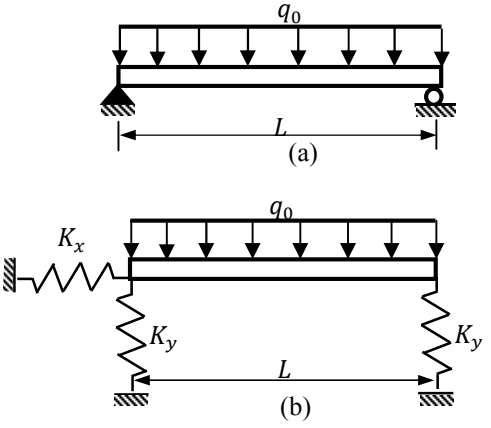

Fig. 2. Geometry of the simplysupported beam.

The analytical quasi-static viscoelastic solution based on TBT of this problem can be expressed as

$$w_{max} = \left(\frac{5qL^4}{384I} + \frac{5qL(1+v)}{8\kappa_s A}\right) D(t) \qquad (22)$$

On the other hand, the semi analytical elastodynamic solution can be written as

$$w_n(x,t) = \sum_{j=1}^{n} \Lambda_j \sin\left(\frac{j\pi x}{L}\right)\left(1 - \cos\left(\eta_j t\right)\right) \qquad (23a)$$

where

$$\Lambda_j = \left\{\frac{q\sqrt{\frac{2}{L}}\left(\sqrt{\frac{2}{L}} \times \frac{L}{j\pi}\right)}{\left(\frac{j\pi}{l}\right)^4 EI}\right\}\left(1 - cos(j\pi)\right)$$

$$and\ \eta_j = \left(\frac{\left(\frac{j\pi}{l}\right)^4 (EI)}{\rho A\left\{1 + \left(\frac{EI}{k_s GA}\right)\left(\frac{j\pi}{l}\right)^2\right\}}\right)^{1/2} \qquad (23b)$$

The time responses for VE and Elbehaviors for quasistatic and dynamic analyses for both simply supported (S-S) and the restrained supported beam with large values of the spring stiffness (flex. joint) are illustrated in Fig. 3. It is shown that good agreement is noticed between both numerical and analytical solutions. Moreover, both S-S and flexible joint analyses result in the same response for both elastic and viscoelastic behavior.

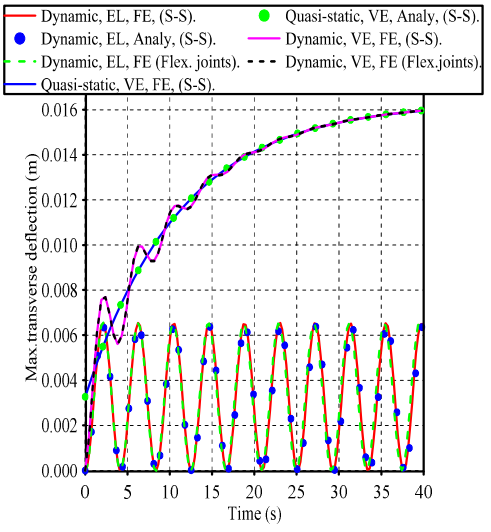

Fig.3. Variation of the maximum deflection with time.

6. Numerical results

In this section the applicability of the proposed procedure is demonstrated. The transient response of double wishbone suspension system under different road irregularities at different values of vehicle speed for different material behavior is investigated. Both step and sine wave road bump profiles are considered. The time dependency of the transverse deflection of the most critically load point on the lower control arm for elastic, viscoelastic, viscous, as

well as proportional damping cases are investigated. Exploiting the symmetry of the vehicle, only a quarter car model is simulated, as shown in Fig. 1.The geometrical and material characteristics used in simulation are summarized in Table 1.

Table 1. The physical properties of the suspension elastic model.

Parameter	Value
$\boldsymbol{E}$ (GPa), (Elastic suspension links)	210
$\boldsymbol{E_\infty}$ (GPa), (VE suspension links)	42
$\boldsymbol{E_1}$ (GPa), (VE suspension links)	168
$\boldsymbol{\rho_v}$ (s), (VE suspension links)	1.0
$\boldsymbol{E}$ (GPa), (chassis and tire axle)	1050
ρ, kg/m3, (chassis and suspension links)	7830
$\boldsymbol{K_s}$ (N/mm), (Strut stiffness)	340
$\boldsymbol{K_{tire}}$ (N/mm), (Tire stiffness)	235
$\boldsymbol{K_x}$ (N/mm), (flex. Joint)	17.544×10^{7}
$\boldsymbol{K_y}$ (N/mm), (flex. Joint)	17.544×10^{7}
$\boldsymbol{K_t}$ (N/mm), (flex. Joint)	19.737×10^{4}
$\boldsymbol{Am^2}$	6×10^{-4}
$\boldsymbol{Im^4}$	12×10^{-8}
$\boldsymbol{C_v}$ (N.s/m)	4×10^{4}
$\boldsymbol{\xi}(-)$	75×10^{-4}

6.1. Road excitation pattern

The road bumps which acts as the system excitation results in vertical vibrations in the whole vehicle body. Both step and sinusoidal road irregularity profiles are considered to study the effect of these profiles on the dynamic characteristics of the suspension systems. Variations of both step and sinusoidal road bump profiles having a same peak with the horizontal distance are shown in Fig. 4, Güler[2006].

Variation of the road bump profile with time at different vehicle speed for both sinusoidal and step road bum profiles is depicted in Figs. 5; respectively.

It is noticed that , the time interval required to pass over the road decreases as the vehicle speed increases and vise- versa. On the other hand, for the considered vehicle speeds, the same peak is reached for the two profiles.

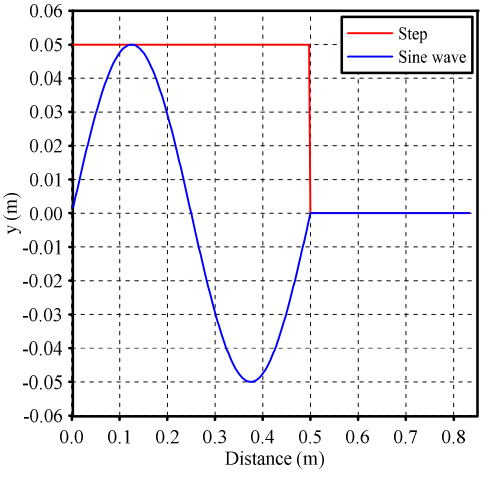

Fig. 4. Variation of the sinusoidal and step road profiles with the horizontal distance.

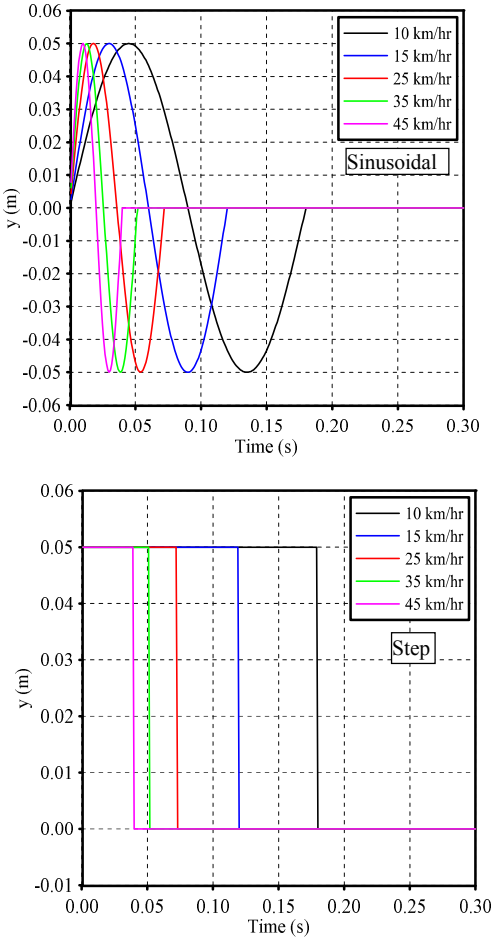

Fig. 5. Variation of the road profile with the vehicle travelling speed for Sinusoidal and Step road profiles.

6.2 Dynamic response

Within this section the vertical displacement and the resultant stress of the critically loaded pointin thelower control arm for different material behavior at different vehicle travelling velocity are investigated. Moreover, effects of both external and internal damping characteristics on the dynamic response are also investigated.

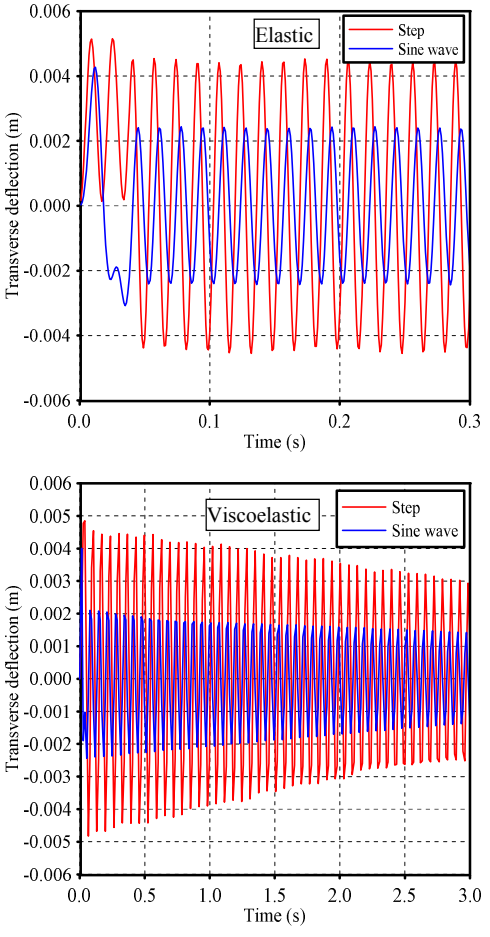

Fig.6. Variation of the transverse displacement with time for both step and sinusoidalroad bumps for elastic and viscoelastic behavior respectively.

6.2.1 Effect the bump profile on the dynamic response

Variation of the maximum vertical deflection at the point P, for both elastic and viscoelastic arm for both step and sinusoidal bump profiles at a travelling speed of 45 km/hr. are represented in Figs. 6. It is noticed both elastic and viscoelastic arms have the same instantaneous response. With time marching, the elastic response oscillates with constant vibration amplitude while the viscoelastic is decaying continuously due to the algorithmic damping of the viscoelastic material. Comparing between the dynamicvertical deflections results from the two road profiles, it is noticed that thestep road profile results in higher values of the maximum vertical deflection amplitude than that obtained forsinusoidal one during loading and unloading intervals.

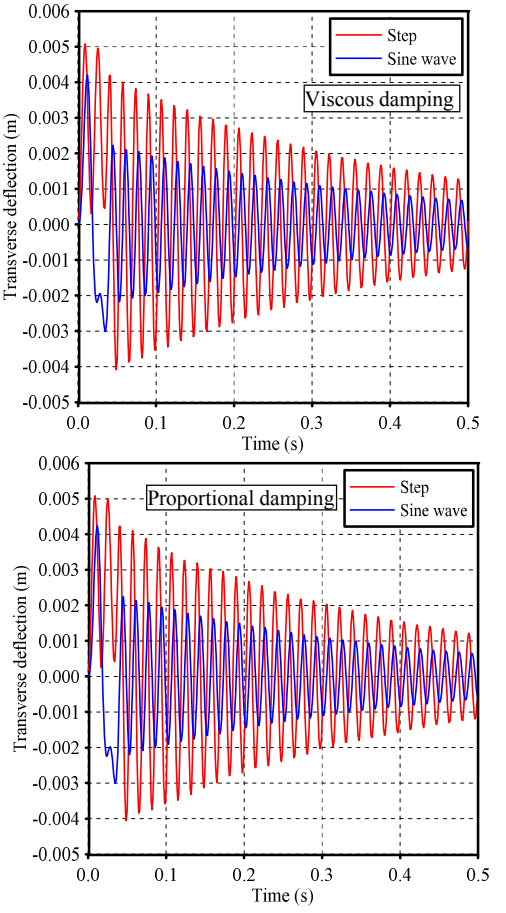

Fig.7.Variation of the transverse displacement with time for both step and sinusoidalroad bumpsfor viscous and proportional damping behavior.

Variations of the maximum transverse deflection with time for both viscous and proportional damping behaviors are shown in Fig. 7. It is noticed that, at the considered values of both the damping factor, ξ and the viscous damping constant, almost the same maximum vertical deflection is detected for the two damping models which is characterized by a rapid decaying rate. So these damping models are not

recommended in the higher vibration modes. Also, higher vibration amplitudes are detected for the step bump profile compared with that obtained for the sinusoidal one.

6.2.2 *Effect of vehicle speed on the dynamic response*

Throughout this section, the dynamic response of the lower control arm is investigated for the following travelling vehicle velocities; 10, 15, 25, 35, and 45 km/hr. considering sinusoidal road bump profile. Variations of the maximum vertical deflection at point P with time at different travelling speeds forboth elastic and viscoelastic material behavior are depicted in Figs. 8.

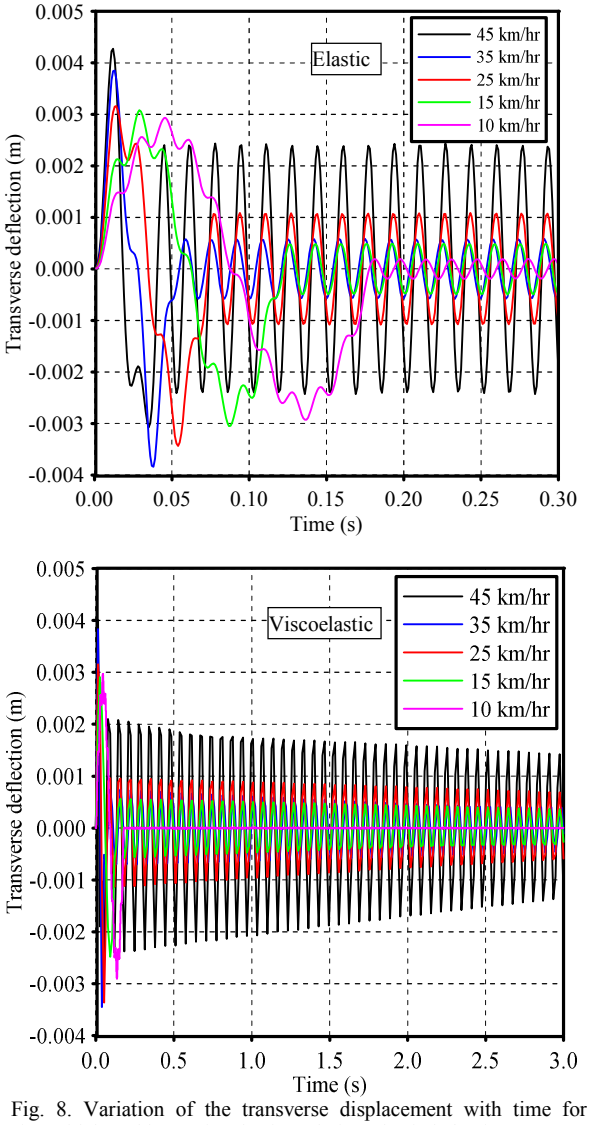

Fig. 8. Variation of the transverse displacement with time for sinusoidal road bump for elastic and viscoelastic behaviors.

It is noticed that, both the maximum oscillation peak of the resulting vibratory motion and the time required to be reached are greatly affectedby the vehicle travelling speed. The maximum amplitude is observed at the maximum travelling speed while the time required to reach the maximum amplitude is increased with decreasing the travelling speed.It is depicted that, during both loading and unloading intervals the maximum oscillation amplitude is detected at the maximum travelling speed and vice versa.Comparing with the corresponding elastic response, the viscoelastic transverse deflection is continuously decaying with time due to the material damping whilethe elastic response proceeds with a constant vibration amplitude for all travelling speeds.

Dependency of the maximum vertical deflection for both viscous and proportional damping behavior is illustrated in Fig. 9.

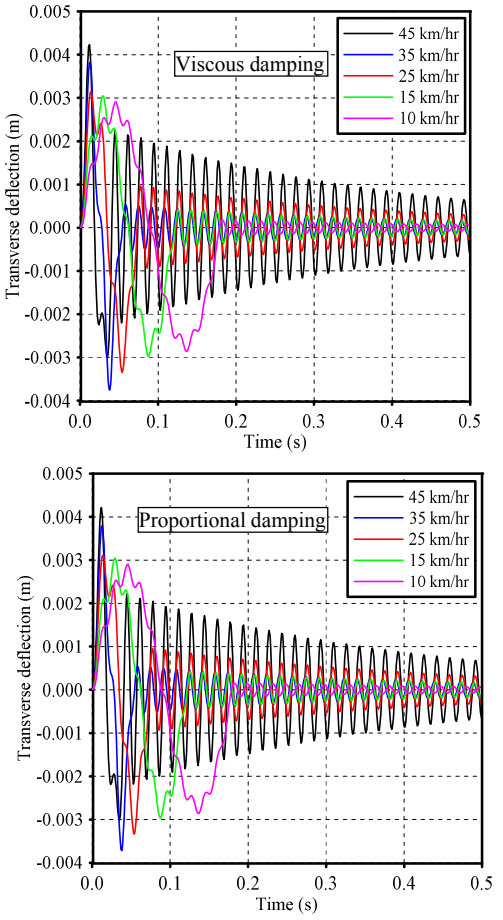

Fig. 9.Variation of the transverse displacement with time for sinusoidalroad bump for viscous and proportional damping behavior.

According to the selected values of the damping factor and the viscous damping constant, almost the same response is detected for both the two damping behaviors. Additionally, comparing with all considered values of the vehicle speed, the smallest amplitude is detected at the smallest velocity and it takes larger time to be reached.

6.2.3 Effect of the viscous damping constant on the dynamic response

Throughout this section, the dynamic response of the lower control arm is studied for the following viscous damping coefficient; $0.25\boldsymbol{C_v}$, $0.5\boldsymbol{C_v}$, $1.0\boldsymbol{C_v}$, $2.0\ \boldsymbol{C_v}$,and $10.0\boldsymbol{C_v}$.Variation of the maximum vertical deflection at different values of the viscous damping constant is illustrated in Fig. 10. It is noticed that during the loading and unloading intervals, the amplitude of oscillation is increased with decreasing the viscous damping constant. On the other hand, the decaying rate is increased with increasing it while the time required to reach the steady state values of the vertical deflection is decreased.

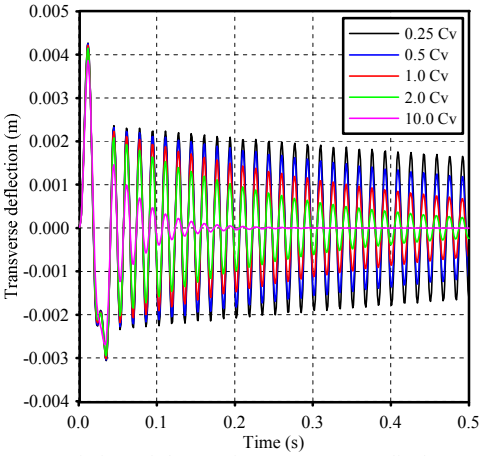

Fig. 10. Variation of the maximum transverse displacement with time at different values of the viscous damping constant.

6.2.4 Effect of the viscoelastic relaxation time on the dynamic response

Within this section,the dynamic response of the lower control arm is investigated for different values of the relaxation time; 0.25 ρ_v, *0.5* ρ_v, 1.0 ρ_v, 1.5 ρ_v, and 2 ρ_v.The time dependency of the maximum vertical deflection of the viscoelastic material behavior at different values of the relaxation time is shown in Fig. 11. It is noticeable that the same instantaneous response is detected for all values of the relaxation time. On the other hand the decaying rate of the vertical deflection is increased with decreasing the viscoelastic relaxation time and consequently, the time required to reach the steady state amplitude is decreased with decreasing the relaxation time.

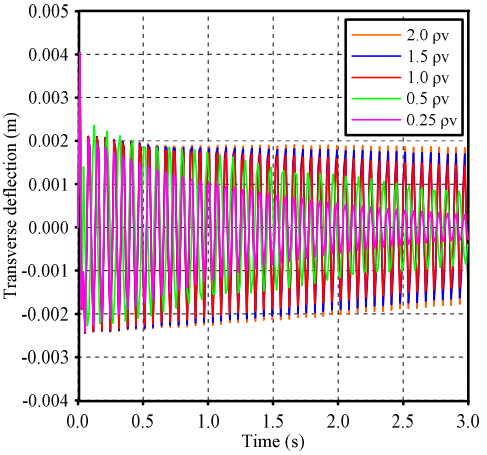

Fig. 11. Variation of the maximum vertical deflection for viscoelastic behavior at different values of the relaxation time.

7. Concluding Remarks

Finite element model is developed to investigate the dynamic response of double wishbone suspension systems considering both links and joints flexibilities. Plane frame element based on TBT is adopted to consider the flexibility of links while the revolute joint element developed in ANSYS is considered for joint flexibility. Both internal and external damping behaviors are considered. The proposed numerical methodology is checked by comparing the obtained results with the developed analytical solution and good agreement is noticed. Parametric studies are conducted to illustrate the applicability of the proposed procedure.Effects of the road irregularity configurations, the vehicle travelling speed, as well as the material damping on the dynamic characteristics of the double wishbone suspension system are investigated. The following remarks are concluded:

1- Bump configuration affects both the instantaneous and the stead state amplitude of the resulting oscillatory motion. The step road profile results in higher amplitudes compared with that obtained from the corresponding sinusoidal one.
2- Vehicle travelling speedgreatly affectsthe dynamic behavior of the double wishbone suspension system. The maximum amplitude is increased with increasing vehicle speed

while the time required to reach this amplitude is increased with decreasing speed.

3- The time required to reach the steady state amplitude is decreasing by increasing the viscous damping coefficient.

4- Increasing the viscoelastic relaxation time results in decreasing the value of the steadystate amplitude and the time required to reach it.

References

[1] J. Reimpell, H. Stoll, and J. W. Betzler," the automotive chassis: engineering principles, 2nd edition "Butterworth-Heinemann, Woburn, Massachusetts, 2001.

[2] R. N. Jazar, "Vehicle dynamics: theory and application, 3rd edition", Springer, 2017.

[3] M.Blundell, and D.Harty, "Multibody systems approach to vehicle dynamics.2nd edition", Elsevier Ltd, 2015.

[4] X.Cheng, and Y.Lin, "Multi objective robust design of the double wishbone suspension system based on particle swarm optimization", The Scientific World Journal, 2014.

[5] A.Rutci, "Failure analysis of a lower wishbone", In Special issue of the International Conference on Computational and Experimental Science and Engineering Vol. 128, 2015.

[6] A. M.Patil, A. S.Todkar, R. S. Mithari, and V. V. Patil, "Experimental& Finite Element Analysis of Left Side Lower Wishbone Arm of Independent Suspension System", IOSR Journal of Mechanical and Civil Engineering, pp. 43-48, 2013.

[7] Dehkordi. H. Banitalebi, "Vibration and force analysis of lower arm of suspension system", Doctoral dissertation, Université du Québec à Chicoutimi, 2014.

[8] S. Azadi, and F. Forouzesh, "Non-linear dynamic analysis of automotive suspension system incorporating rubber bump stops". Proceedings of the Institution of Mechanical Engineers, Part D: Journal of Automobile Engineering, 225(8), 1023-1032, 2011.

[9] K. V. Reddy, M. Kodati, K. Chatra, and S.Bandyopadhyay, "A comprehensive kinematic analysis of the double wishbone and MacPherson strut suspension systems", Mechanism and Machine Theory Vol. 105, pp. 441-470, 2016.

[10] K. P. Balike, S. Rakheja, and I. Stiharu, "Development of kineto-dynamic quarter-car model for synthesis of a double wishbone suspension", Vehicle System Dynamics Vol. 49(1-2), pp. 107-128, 2011.

[11] E. Tanik, and V. PARLAKTAŞ,"On the analysis of double wishbone suspension", Journal of Advanced Mechanical Design, Systems, and ManufacturingVol. 9, No. 3, JAMDSM0037-JAMDSM0037, 2015.

[12] A. Bhoraskar, A. Fartyal, and P.Sakthivel, "Analysis of the Double Wishbone front suspension system", In Nascent Technologies in Engineering (ICNTE), International Conference on pp. 1-5. IEEE, 2017.

[13] C. Kavitha, S. A. Shankar, K. Karthika, B. Ashok, and S. D. Ashok, "Active camber and toe control strategy for the double wishbone suspension system", Journal of King Saud University-Engineering Sciences, 2018.

[14] H., Kanchwala, and A. Chatterjee, "A generalized quarter car modelling approach with frame flexibility and other nonlocal effects",Sādhanā Vol. 42, No 7, pp. 1175-1192, 2017.

[15] M. Pourshams, M. I. Mokhlespour, A. Keshavarzi, and M. H. Talab, "Design, Analysis and Manufacturing a Double Wishbone Suspension System with Variable Camber Angle by Pneumatics Mechanism", In ASME 2011 International Mechanical Engineering Congress and Exposition, pp. 477-483. American Society of Mechanical Engineers, 2011.

[16] V. K. Soo, P. Compston, and M.Doolan, "Interaction between new car design and recycling impact on life cycle assessment", Procedia CIRP Vol. 29, pp. 426-431, 2015.

[17] N. A. Kadhim, N. Nikabdullah, S. Abdullah, and A. K. Ariffin, "Automotive Lower Suspension Arm: Experimental and Simulation Durability Assessment", Academy Publish. Org-Vehicle Engineering, pp. 53-74, 2011.

[18] B. Gadade, and R. G. Todkar, "Design, analysis of A-type front lower suspension arm in commercial vehicle", International Research Journal of Engineering and Technology, Vol. 2, No .7, pp. 759-766, 2015.

[19] A. Abd_Elsalam, M. A. El-Gohary, and H. A. El-Gamal, "Simulation of Nonlinear Quarter Car Suspension System with and without Tire Damping", 2016.

[20] C. O. Ijagbemi, B. I. Oladapo, and H. M. Campbell, "Design and simulation of fatigue analysis for a vehicle suspension system (VSS) and its effect on global warming", Procedia engineering Vol. 159, pp. 124-132, 2016.

[21] M. Sridharan, andDr. S. Balamurugan, "Design and Analysis of Lower Control ARM", International Journal of Innovative Research in Science, Engineering and Technology Vol. 5, No 4, pp. 6510-6528 , 2016.

[22] U. A. Ramesh, D. Siddhartha, R. A. Sethu, N. Ramanan, and V.Karthi, "Modeling and Analysis of Lower Wishbone for Independent Suspension System for Commercial Vehicles", Journal of Chemical and Pharmaceutical Sciences Vol. 2, pp. 166-168, 2017.

[23] J. N. Reddy,"Theory and analysis of elastic plates and shells. 2nd ed.", Boca Raton, FL: CRC Press; 2007.

[24] J. N. Reddy,"Microstructure-dependent couple stress theories of functionally graded beams", J MechPhys Solids Vol. 59, pp. 2382–99, 2011.

[25] E. Carrera, G. Giunta, and M.Petrolo, "Beam Structures, Classical and Advanced",A John Wiley & Sons, Ltd., Publication, 2011.

[26] W. N. Findley, and F. A. Davis, "Creep and relaxation of nonlinear viscoelastic materials", Courier Corporation, 2013.

[27] O.Martin, "A modified variational iteration method for the analysis of viscoelastic beams", Applied Mathematical Modelling Vol. 40, No (17-18), pp. 7988-7995, 2016.

[28] D. J. Inman, "Engineering vibration. Pearson. 4th. ed.", Pearson Education, 2014.

[29] L.Weili, X. Yong, and W.Shun, "Vibration of Timoshenko beam on hysteretically damped elastic foundation subjected to moving load", Science China, Physics, Mechanics & Astronomy Vol. 58, No 8, 084601, doi: 10.1007/s11433-015-5664-9, 2015.

[30] A. Capsoni, G., M. Viganò, and K. Bani-Hani, "On damping effects in Timoshenko beams", International Journal of mechanical sciences Vol. 73, pp. 27-39, 2013.

[31] P. Kohnke, "ANSYS Theory Reference", Release 5.5 ANSYS. Inc., Canonsburg, 1997.

[32] A. S. Da Costa Azevêdo, A. C. A. Vasconcelos, andS. dos Santos Hoefel, "Dynamic analysis of elastically supported Timoshenko beam", RevistaInterdisciplinar de PesquisaemEngenharia-RIPE Vol. 2, No. 34, pp. 71-85, 2016.

[33] D. Güler,"Dynamic analysis of double wishbone suspension",Master's thesis, İzmir Institute of Technology, 2006.